Available online at www.derpharmachemica.com

Scholars Research Library

Der Pharma Chemica, 2012, 4 (1):544-551
(http://derpharmachemica.com/archive.html)

ISSN 0975-413X
CODEN (USA): PCHHAX

Bio-physiochemical characterization of anticancer nano-ceramic polymer scaffold for bone grafting

Hanan H. Beherei[1,2,*], Mohamed S. Abdel-Aal[1,3], Abdallah A. Shaltout[1,3], A. El-Magharby[1, 4]

[1]*Faculty of Science, Taif University, 21974 Taif, P.O. Box 888, Saudi Arabia*
[2]*Biomaterials Department, National Research Center, El Behooth Str., 12622 Dokki, Cairo, Egypt*
[3]*Spectroscopy Department, Physics Division, National Research Center, El Behooth Str., 12622 Dokki, Cairo, Egypt*
[4]*Refractory and Ceramics Department, National Research Center, El Behooth Str., 12622 Dokki, Cairo, Egypt*

Abstract

The main challenge of the implant technology used for bone cancer therapy is the development of a new generation of bioactive implants with enhanced multifunctional roles such as bone graft material and hyperthermia generator. The aim of this work is to prepare nano-ceramic fillers-based hydrogel biopolymer as spongy bone substitute with high biocompatibility, bioactivity, and osteoconductivity. The possibility of preparing a series of nano - brushite/ γ -Fe_2O_3 / hydrogel biopolymer scaffolds was demonstrated as a new generation of bone graft and tissue engineering. The improvement of bioactivity properties of new scaffolds carried out by adding 5, 10 and 15 wt% of nano - γ - Fe_2O_3 to 95, 90 and 85 wt% of nano-brushite respectively. The developed nano-ceramic phases were investigated by TEM and XRD. The prepared scaffolds were investigated by pore analysis and mechanical properties before immersion in simulated body fluid (SBF). Due to the applied electromagnetic field the magnetite induces hyperthermia and measuring temperature increases. The in-vitro behavior was assessed via measurement of calcium and phosphorus ions in SBF. The obtained results revealed that the γ - Fe_2O_3 enhanced the bioactivity properties of the prepared scaffolds by formation of bone-like apatite on surfaces of the scaffolds, especially at high ratio of γ- Fe_2O_3 (15%) according the measurement of calcium and phosphorous. The mechanical properties of the composites are within the range of cancallous bone. The combination of osteoconductivity properties of these scaffolds confirms excellent mechanical properties which leads to the development of high strength medical scaffolds with appropriate bioactivity and anticancer activity.

Keywords : Nano-brushite, Nano- γ -Fe2O3 , Biopolymer, Anticancer, In-vitro, Scaffolds.

INTRODUCTION

In the tissue engineering approach, with the target of repairing large bone defects, a porous scaffold (artificial extracellular matrix) is needed to accommodate cells, guide their growth and tissue regeneration in three dimensions[1].

Superparamagnetic iron oxide nano-particles including Fe_3O_4 magnetite and γ-Fe_2O_3 maghemite have great potential for various biomedical applications. They include magnetic resonance imaging (MRI) contrast enhancement, targeted drug delivery, hyperthermia, catalysis, biological separation, biosensors, and diagnostic medical devices [2–5].

Moreover, most of them involve invasive heat application. It has been reported that ferro or ferromagnetic particles can heat the tumor locally without damaging normal tissue. These magnetic particles are easily incorporated into a tumor and generate heat under an alternating magnetic field mostly by hysteresis loss. It is known that the heat generation depends mainly on the magnetic properties of the implant, the magnetic field parameters and the characteristics of the tissue. One of the most important requirements in the field of materials for magnetic hyperthermia is to tailor the desired magnetic properties of the implant. The mechanism of heat production depends mainly on the microstructure of the implanted magnetic material (crystals structure, magnetic domain structure, magnetic anisotropy, residual stress, particles size, grain shape and crystals imperfections). Therefore, by controlling the magnetic properties of implanted materials we can adjust the heat generation under an oscillating magnetic field. Ferrimagnetic biomaterials are potential candidates for magnetic induction hyperthermia. This method consists of heating target tissues to temperatures between 41° to 46°C. At these temperatures, malignant cells are destroyed whereas healthy cells do not undergo important or nonreversible damage. This effect is related to the tumor hypoxic environment, which leads to acidic conditions with the thermal treatment and to the subsequent cytoplasmatic destruction. Although the biologic effects are very positive, the lack of thermal homogeneity for the treatment of deep-sited tumors obligates one to use implanted thermoseeds or ferrofluids. The problem becomes more complicated when the tumor is located in the bone tissue. The concealing the bone tissue loss is necessary after surgical removal. Moreover, a subsequent antitumor treatment needs in order to avoid recurrence[2-5].

Hydrogels are appealing scaffold materials due to their high water content, good biocompatibility and consistency similar to soft tissue. They play an important role in several applications including tissue engineering and controlled delivery of therapeutic agents. The simplest and the most convenient approach of these applications will be used with the polymer-cell or drug entity into the body with a minimally invasive manner. Naturally derived hydrogels resemble the nature extracellular matrix because they have the potential to orient the migration, growth and organization of cells during tissue regeneration. In addition, they can use for wound healing, stabilization of encapsulated and transplanted cells [6]. It is well known that alginate is a natural biomacromolecule isolated from seaweed and bacteria. It is consisting of (1 → 4) linked β-Dmannuronate (M) and its C-5 epimer α-L-guluronate (G) residues arranged in blocks of M fragments, G fragments and alternating G and M fragments [6]. Therefore, important to produced material that can forms as well characterized hydrogels by adding divalent cations (except Mg^{2+}) under physiological conditions [7]. The use of alginate scaffolds in tissue-engineering applications is limited owing to their weak mechanical properties, lack of cellular interactions and uncontrollable degradation [8]. For these reasons, covalent crosslinking has been investigated in order to impart controlled mechanical properties to the alginate hydrogels [9].

Brushite-forming calcium phosphate bone cements have the advantage of being resorbable in comparison to hydroxyapatite (HA)-forming cements but suffer in application from their fast, water-consuming setting reaction and their low mechanical strength [10,11].

Preparation of nano - brushite filler powder was performed. The loading of nano – brushite and γ-Fe_2O_3 powders onto the polymeric matrix in scaffolds for improving the bioactivity, biodegradation as well as the mechanical properties and anticancer effect were carried out. The characterization of the prepared biocomposites to verify the homogeneity between two matrices, and in vitro test was performed, to insure the formation of apatite layer onto the surface of the materials.

MATERIALS AND METHODS

2.1. Materials

The polymer material used in this study was alginate. Alginic acid sodium salt from brown algae with medium viscosity (weight-average molecular weight 900 kDa) was purchased from Sigma-Aldrich, Steinheim, Germany. All other starting materials used for preparing the scaffolds were supplied from Sigma.

2.2. Preparation of brushite

Synthesis of brushite was prepared with flat-plate-shaped crystals. The synthesis procedure consisted of two preparing solutions(A and B). The first solution(solution A) was prepared by dissolving 0.825 g of KH_2PO_4 in 700 mL of distilled water, followed by adding 3.013 g of Na_2HPO_4. The final solution was a clear solution of pH 7.5 at room temperature. The second solution (solution B) was prepared by dissolving 4.014 g of $CaCl_2 \cdot 2H_2O$ in 200 mL of distilled water with pH 6.4. Solution B was then rapidly mixed with to solution A and the precipitates formed were aged for 80 min at room temperature using continuous stirring at 500 rpm and the final solution has pH = 5.3. Solids recovered by filtration from their mother liquors were dried overnight at 65 °C and it was fired at 700°C to obtain 3.28 g of flat plate shaped brushite powders.

2.3. Preparation of Scaffolds

The prepared nano-brushite and Fe_2O_3 were mixed as filler powders and were loaded onto polymeric matrix to make serious of scaffolds as follow:

1. 100% Brushite in the polymeric matrix .
2. 95% Brushite + 5% Fe_2O_3 in the polymeric matrix.
3. 90% Brushite + 10% Fe_2O_3 in the polymeric matrix.
4. 85% Brushite + 15% Fe_2O_3 in the polymeric matrix.

After 2.5 h from polymerization process, a 3.5 of nanopowders were mixed with the polymer mixture and experiment and kept at 40°C in water bath for 30 min to complete the polymerization process. The scaffolds were leaved overnight at room temperature and then the mixture was washed with hot ethanol with stirring for 2 h. The mixture was filtered, collected and dried at 60°C overnight.

The scaffolds were prepared through the solid–liquid phase separation. Solvent extraction was chosen to remove the crystals after phase separation processes. A 30% wt/v solution of hydrogel in chloroform was stirred with the obtained nanopowders for 12 h till a well dispersed homogenous suspension was obtained. The suspension was frozen at −80 °C during 24 h to induce the solid–liquid phase separation of the polymer solution. The solvent was extracted from

the frozen sol–gel nanopowders/ polymer mass by immersion into absolute ethanol at −80 °C, and ethanol was replaced with fresh ethanol each 8 h during two days. After complete extraction of chloroform, ethanol was removed by drying at room temperature to obtain the porous scaffolds. [12].

The phase analysis of the nanoceramic fillers was examined by X-Ray diffractometer (Bruker, Karlsruhe, Germany) equipped with Cu-K radiation. The morphology and particle size of the nano-powders (prepared brushite and γ-Fe_2O_3) were analyzed using TEM (JEM2010, Japan) working at 200 kV.

The scaffolds were tested to determine the effect of polymeric matrix on the mechanical properties of the composites. The average value for each test was calculated for ten replicates to confirm the results. The compressive strength was measured for the prepared composites by using tensile testing machine, Zwick Z010, Germany. The average value for each test was taken for three samples to verify the results. The shape of sample was cylindrical (1 cm × 2 cm), load cell was10 KN and crosshead speed was 10 mm/min.
The size and porosimetric distribution was determined by Hg porosimetry method using a (Zeiss, Germany-device) the used working parameters were as follows: 0–2000 atm, working fluid Hg, sample weight 20 mg.

The scaffolds were soaked in SBF, proposed by Kokubo et al. [13] at body temperature (37°C) and pH = 7.4 for several periods. In briefly, SBF contains ions similar to those in human blood plasma and was prepared by dissolving the following reagent grades: NaCl, $NaHCO_3$, KCl, $K2HPO_4.3H_2O$, $MgCl_2.6H_2O$, $CaCl_2$ and Na_2SO_4 in ion exchanged distilled water. The solution was buffered at pH= 7.4 with Tris (hydroxymethylaminomethane) $[(CH_2OH)_3CNH_2)]$ and 1M hydrochloric acid (HCl). After immersion, the solutions were analyzed by the spectrophotometer (UV-2401PC,UV–VIS recording spectrophotometer, Shimadzu, Japan) using biochemical kits (Techo Diagonstic, USA) to detect the total calcium ions (Ca^{2+}) at □ = 570 nm and phosphorus ions (P) concentration at □ = 675 nm.

Hyperthermia was obtained by due to the interaction of the scaffolds with the electromagnetic field. The magnetic field was created using a horizontal coil and the applied frequency was being 150 kHz.

RESULTS AND DISCUSSION

3.1. Transmission electron microscope (TEM) of nano-fillers.

Figure 1, shows the representative transmission electron microscopy (TEM) image of the prepared pure brushite. It indicates that prepared brushite is composed of nanostructures in flat plate shape . The diameter of the flat plates is between 50 nm and 200 nm, as shown in Figure 1.

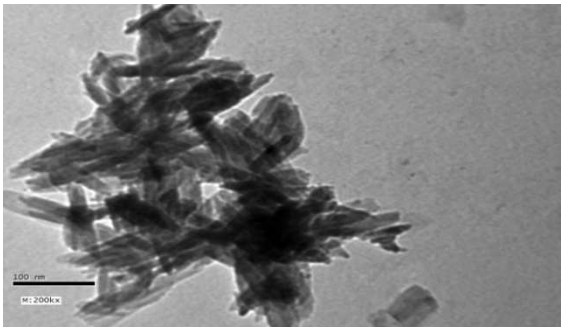

Fig.1.TEM image of prepared pure brushite .

The results indicate that the dispersant has an obvious influence on the morphology and size of brushite particles. It can be concluded that the dispersant may prevent the growth of brushite particles and provide different size distribution.

Figure.2., shows the representative transmission electron microscopy (TEM) image γ- Fe_2O_3 particles. The γ- Fe_2O_3 particles are very spherical uniform size distribution.

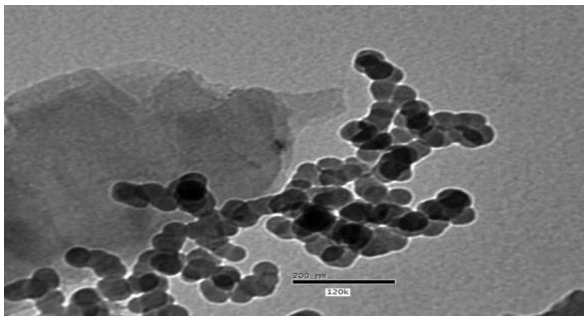

Fig.2. TEM image of γ- Fe_2O_3 particles

3.2. X-Ray diffraction analysis

Figure 3, shows the XRD patterns of pure brushite (B), 95% Brushite+5% Fe_2O_3 (D), 90% Brushite +10% Fe_2O_3 (F) and 85% Brushite+15% Fe_2O_3 (H) respectively.

The obtained patterns of the pure brushite have a well crystalline structure (Figure 3). The diffraction peaks of the crystals are indexed to brushite crystal structure (JCPDS file no. 2-0085), at 2θ equals 11.63, 20.93, 29.27, 30, 50, 34,14,34.41, 41.52 and 50.17 respectively. No characteristic peaks of other calcium phosphate phases or impurities were detected. The intensity of the diffraction peaks indicates that the fillers were well crystallized. The obtained XRD patterns of brushite with different ratios of Fe_2O_3 fillers (D, F and H) indicate a similar crystalline structure with the pure brushite but with lower degree of crystallinity. The presence of maghemite (γ- Fe_2O_3) was detected in the fillers by its characteristic diffraction peaks at 2θ: 30.4, 35.8, 43.6, 54.2 and 57.5 respectively. A difference in the line broadening is also observed. The decreasing of the crystalline structure, indicates the presence of small particles.

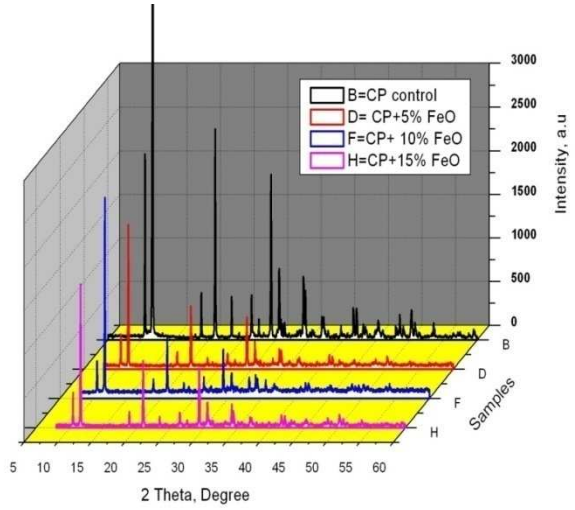

Fig.3. XRD of fillers.

3.3. Pore analysis

The interconnected pore aperture distributions were obtained from mercury intrusion porosimetry (Table 1). Table 1 shows that scaffolds that were formed with 90.2% porosity and exhibited a modal interconnected pore diameter of 90μm for Cp scaffold. The reduced modal pore diameter decreased to 86μm and porosity to 88.34% for F_1 scaffold. 100μm should be a suitable pore size for tissue engineering applications as there appears to be many apertures larger than the mode. From Table 1, the pore characters decrease for F_2 and F_3 scaffold [14 - 16] .

Table (1) :The pore analyses of prepared scaffolds.

Scaffold	Total pore area m^2/g	Av. Pore density µm	Bulk density g/ml	Apparent density g/ml	Total porosity %
Pure Brushite	110	90	0.9	2.43	90.2
95% Brushite+5% Fe_2O_3	98	86	1.35	2.85	88.34
90% Brushite+10% Fe_2O_3	95	84	1.26	2.6	82.11
85% Brushite+10% Fe_2O_3	92	80	1.22	2.15	81.23

3.4. Mechanical properties

Table 2 shows the compressive strength of the prepared scaffolds. The compression test of the composites increases with increasing of the composites that include Fe_2O_3. These results demonstrated that the mechanical properties of porous scaffolds were significantly affected by adding the Fe_2O_3 in the composite. These values should be a suitable for tissue engineering applications.

Table 2, The mechanical properties of prepared scaffolds

Composites	Compressive strength, MPa
Pure Brushite	4
95% Brushite+5% Fe_2O_3	5
90% Brushite+10% Fe_2O_3	9
85% Brushite+15% Fe_2O_3	11

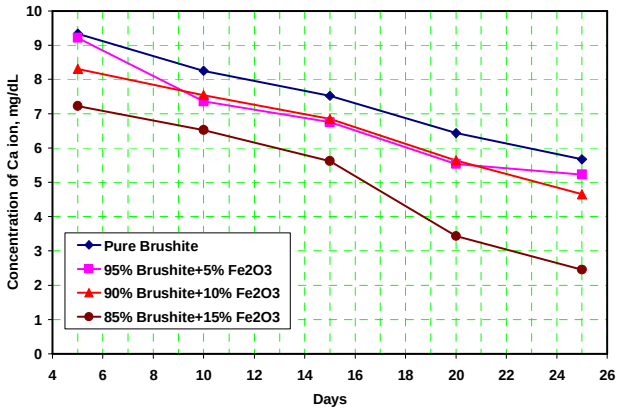

Figure 4. The variations of Ca++ ion concentration with the different scaffolds.

3.5. The in vitro behavior

3.5.1. In vitro test

The concentration of Ca++ ions recorded at different time ranging from 5 to 25 days. Figure 4 illustrates the variations of Ca++ ion concentration with the different scaffolds. It was found that,

the concentration of Ca++ decreases as the ratios of Fe_2O_3 increases. On the other hand, as the time increases the concentration of Ca++ decreases. Therefore, the low value for the three scaffolds compared to the control confirms the deposition of Ca++ ions onto their surfaces. Figure 4 depicts the concentrations of Ca++ ions in the prepared scaffolds in SBF. The result proves the interaction between the scaffolds and the Ca++ ions in SBF via hydrogen bonding.

3.5.2. Phosphorus ions (P)

In the same manner, the concentration of P ions recorded at different time ranging from 5 to 25 days. Figure 5 illustrates the variations of Ca++ ion concentration with the different scaffolds. It was found that, the concentration of P decreases as the ratios of Fe_2O_3 increases. On the other hand, as the time increases, the concentration of P decreases. Therefore, the concentration of P ions postimmersion recorded lower values for the three scaffolds compared to the control denoting the deposition of P ions on the material surface. This is due to the affinity of polymer as cationic polymer to phosphate ions [16]. Therefore, the presence of the nanofillers containing brushite enhances and promotes the deposition of phosphorus ions which is in the favor of apatite layer formation onto its surface.

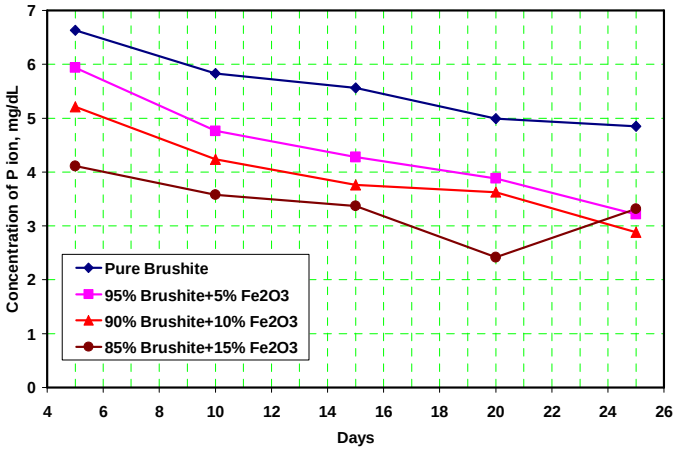

Figure 5, The variations of P ion concentration with the different scaffolds.

3.6. Hyperthermia

The obtained scaffolds materials were analyzed also from the produced hyperthermia point of view. Perior to the measurments, the scaffold materials were kept at 37 °C for 1 h. Afterwards,, the three scaffolds (containing Fe_2O_3) materials were introduced in the electromagnetic field with frequency 150 kHz and the temperature was determined after 10, 20, 30 and 40 min [17].Table 5 illustrates the determined temperature after the different mentioned times. It can be observed that increasing amount of magnetite lead to an increase thermal effect**.**

Table (5): The Temperature (°C) dependence of prepared scaffolds with irradiation time (min) (frequency = 150 kHz)

Scaffolds	Time, min				
	0	**10**	**20**	**30**	**40**
Pure Brushite	37°C	37°C	37°C	37°C	37°C
95% Brushite+5% Fe_2O_3	37°C	38°C	40°C	42°C	43°C
90% Brushite+10% Fe_2O_3	37°C	39°C	42°C	43°C	45°C
85% Brushite+15% Fe_2O_3	37°C	40°C	43°C	45°C	47°C

CONCLUSION

The aim of the present work is to obtain a regenerative scaffolds based on brushite and biopolymer in the presense of different concentration of γ-Fe_2O_3 nanoparticle. The role of γ -Fe_2O_3 is to produce controlled hyperthermia which can be activated by an alternative electromagnetic field at any time after implantation. It was obtained a multifunctional scaffolds material in order to assure bone regeneration and anticancer effect. According to the in vitro behavior, the concentrations of Ca and P ions are inversely proportiaonl with the ratios of Fe_2O_3 and the. Obviously, the scaffold materials containing 5 % γ -Fe_2O_3 cannot produce the necessary hyperthermia; the F_2 and F_3 scaffold with higher content of F_3 (for instance and 10% and 15%) can be successfully used as hyperthermia generator system, the activation time being of about 20–30 min (at 150 kHz)

REFERENCES

[1] M. Braddock, P. Houston, C. Campbell, Ashcroft P. *News Physiol. Sci.* 16 (**2001**) 208–13.
[2] McCarthy JR, Weissleder R. *Adv Drug Delivery Rev* **2008**;60:1241–51.
[3] Salgueirino-Maceira V, Correa-Duarte MA. *Adv Mater* **2007**;19:4131–44.
[4] Gupta AK, Naregalkar RR, Vaidya VD, Gupta M. *Nanomedicine* **2007**;2:23–39.
[5] Veiseh O, Gunn JW, Zhang M. *Adv Drug Delivery Rev* **2010**;62:284–304.
[6] Moe S T, Dragel K I, Smidsrød O. (**1995**) Alginates In: Stephen, A. M., (Eds), Food polysaccharides and their applications. New York:Marcel Dekker.
[7] Ji M. (**1997**) The chemistry of seaweed. Beijing: Science Publishing House.
[8] Bouhadir K H, Mooney D J. (**2002**) New York: Academic Press
[9] Eiselt P, Lee K Y, Mooney D J. (**1999**) *Macromolecules* 32: 5561-5566.
[10] Bohner M, Gbureck U, Barralet JE. *Biomaterials* **2005**;26:6423–9.
[11] Bohner M. *Injury* **2000**;31:37–47.
[12] J. He, D. Li, Y. Liu, B. Yao, B. Lu, Q. Lian. *Polymer* 48 (**2007**) 4578-4588.
[13] T. Kokubo, H. Kim, M. Kawashita, *J. Biomater*. 24 (**2003**) 2161.
[14]J. Wang, W.Fu, D. Zhang, Xixun Yu, J. Li and C. Wan., *Carbohydrate Polymers* 79 (**2010**) 705–710.
[15] A.Hawkins a, T.Milbrandt, D. Puleo, J. Hilt., *Acta Biomaterialia* 7 (**2011**) 1956–6194.
[16] A. Butscher, M. Bohner, S. Hofmann, L. Gauckler and R. Müller., *Acta Biomaterialia* 7 (**2011**) 907–920
[17] R. Prucek , J.Tucek, M. Kilianová, A.Panácek, L.Kvítek, J. Filip, M. Kolá_ c,K.Tománková, R. Zboril, *Biomaterials*, 32 (**2011**) 4704e4713